Title

Evaluation of the diagnostic yield of dental radiography and cone-beam computed tomography for the identification of dental disorders in small to medium-sized brachycephalic dogs

Journal

American Journal of Veterinary Research, 79(1)

ISSN

0002-9645

Authors

Döring, S
Arzi, B
Hatcher, DC
et al.

Publication Date

2018

DOI

10.2460/ajvr.79.1.62

Peer reviewed

Evaluation of the diagnostic yield of dental radiography and cone-beam computed tomography for the identification of anatomic landmarks in small to medium-sized brachycephalic dogs

Sophie Döring DVM
Boaz Arzi DVM
Catherine R. Barich DVM
David C. Hatcher DDS, MSc
Philip H. Kass DVM, PhD
Frank J. M. Verstraete Dr Med Vet

Received December 13, 2016.
Accepted May 8, 2017.

From the Dentistry and Oral Surgery Service, William R. Pritchard Veterinary Medical Teaching Hospital (Döring, Barich), and the Departments of Surgical and Radiological Sciences (Arzi, Hatcher, Verstraete) and Population Health and Reproduction (Kass), School of Veterinary Medicine, University of California-Davis, Davis, CA 95616; and Diagnostic Digital Imaging Center, 99 Scripps Dr, No. 101, Sacramento, CA 95825 (Hatcher). Dr. Döring's present address is Tierklinik Oberhaching, Bajuwarenring 10, 82041 Oberhaching, Germany.

Address correspondence to Dr. Verstraete (fjverstraete@ucdavis.edu).

OBJECTIVE
To evaluate the diagnostic yield of dental radiography (Rad method) and 3 cone-beam CT (CBCT) methods for the identification of predefined anatomic landmarks in brachycephalic dogs.

ANIMALS
19 client-owned brachycephalic dogs admitted for evaluation and treatment of dental disease.

PROCEDURES
26 predefined anatomic landmarks were evaluated separately by use of the RAD method and 3 CBCT software modules (serial CBCT slices and custom cross sections, tridimensional rendering, and reconstructed panoramic views). A semiquantitative scoring system was used, and mean scores were calculated for each anatomic landmark and imaging method. The Friedman test was used to evaluate values for significant differences in diagnostic yield. For values that were significant, the Wilcoxon signed rank test was used with the Bonferroni-Holm multiple comparison adjustment to determine significant differences among each of the 6 possible pairs of diagnostic methods.

RESULTS
Differences of diagnostic yield among the Rad and 3 CBCT methods were significant for 19 of 26 anatomic landmarks. For these landmarks, Rad scores were significantly higher than scores for reconstructed panoramic views for 4 of 19 anatomic landmarks, but Rad scores were significantly lower than scores for reconstructed panoramic views for 8 anatomic landmarks, tridimensional rendering for 18 anatomic landmarks, and serial CBCT slices and custom cross sections for all 19 anatomic landmarks.

CONCLUSIONS AND CLINICAL RELEVANCE
CBCT methods were better suited than dental radiography for the identification of anatomic landmarks in brachycephalic dogs. Results of this study can serve as a basis for CBCT evaluation of dental disorders in brachycephalic dogs. (*Am J Vet Res* 2018;79:54–61)

Brachycephalic dogs are represented by more than 25 breeds, which range from small (eg, Pekingese) to medium-sized (eg, Boxer) to large (eg, English Mastiff) dogs. All of these breeds are predisposed to developmental disorders of orofacial structures and multiple dental disorders.[1–6] Brachycephaly can be confirmed by measurement of the skull and calculation of the skull index.[7] Currently, dental radiography is the only imaging modality regularly used when diagnosing dental disorders in brachycephalic dogs.

Full-mouth dental radiographs (14 standard intraoral projections) represent the diagnostic criterion-referenced standard in veterinary dentistry.[8,9] Although it is known that 2-D images of a tridimensional structure lead to projection errors and errors of identification,[10] these shortcomings are accepted because full-mouth dental radiography still provides sufficient information to assess dental pathological conditions in dogs with a mesaticephalic or dolichocephalic skull configuration. However, the interpretation of dental radiographs may be more difficult for brachycephalic dogs because of overlapping of anatomic structures, crowding of teeth, and rotation of teeth.

In human dentistry, CBCT is commonly used when conventional radiography cannot supply satisfactory diagnostic information.[11–13] With advanced imaging software, CBCT provides transverse, sagittal, and dorsal slices as well as multiplanar reconstructions (cross sections), curved planar reformations (simulated distortion-free panoramic images), and indirect volume renderings (tridimensional renderings) in tooth and bone mode.

ABBREVIATIONS
CBCT Cone-beam CT

The objective of the study reported here was to evaluate the use of conventional full-mouth intraoral dental radiography and CBCT for the identification of predefined clinically relevant anatomic landmarks of the orofacial region in small to medium-sized brachycephalic dogs. For this purpose, 26 predefined anatomic landmarks were evaluated by use of both imaging modalities. Furthermore, to characterize the diagnostic method that was most useful among the CBCT methods, the 3 software modules provided by the CBCT software were evaluated separately. We hypothesized that CBCT images would yield more detailed information and would be better suited than dental radiographs for use in identifying anatomic landmarks in brachycephalic dogs.

Materials and Methods

Animals

All client-owned small to medium-sized brachycephalic dogs (confirmed by use of the skull index) admitted to the Dentistry and Oral Surgery Service at the University of California-Davis for evaluation and treatment of oral pathological conditions between August 2014 and October 2015 for which full-mouth dental radiographs and CBCT scans of the skull were obtained were included in the study. Informed consent was obtained from each owner, and the study was conducted with approval of the University of California-Davis Institutional Animal Care and Use Committee and the Clinical Trials Review Board.

Image acquisition

Dogs were anesthetized, and dental radiography and CBCT were performed. Full-mouth dental radiographs were obtained by use of a digital intraoral imaging system[a,b] at 60 kVp and 7 mA with an exposure time of 0.12 to 0.25 seconds (depending on size of the patient and location of the evaluated teeth). This system yielded a resolution of up to 18 line pairs/mm, which equated to a pixel size of 55.5 µm. Radiographic images included the standard series of views in accordance with American Veterinary Dental College guidelines.[14] A CBCT unit[c] was used to obtain images. Field of view was 15 X 12 cm or 18 X 16 cm (depending on size of the dog's skull), and serial slices of the skull were obtained with a scan time of 18 or 24 seconds, which resulted in a voxel size (slice thickness) of 150 or 250 µm, respectively.

Image evaluation and scoring

Dental radiography (Rad method) and 3 CBCT software modules (reconstructed panoramic views [Pano method], serial CBCT slices and custom cross sections [Slices method], and tridimensional rendering [3-D method]) were evaluated separately for their usefulness in identification of 26 predefined clinically relevant oral anatomic landmarks **(Appendix)**. Images were examined on medical-grade flat-screen monitors[d] by use of commercially available software,[e,f] and each method was scored separately for each landmark by a third-year resident in a veterinary dentistry training program (SD), 2 board-certified veterinary dentists (BA and FJMV), and a board-certified human oral radiologist (DCH).

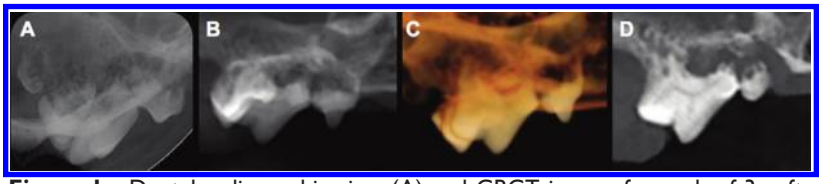

Figure 1—Dental radiographic view (A) and CBCT images for each of 3 software modules (reconstructed panoramic views [Pano method; B], tridimensional rendering [3-D method; C], and serial CBCT slices and custom cross sections [Slices method; D]) that provide examples of the inability to identify (grade = 0; scale, 0 to 3) the entire right maxillary fourth premolar tooth because of overlapping of adjacent teeth and the zygomatic arch as well as dental pathological changes in a brachycephalic dog.

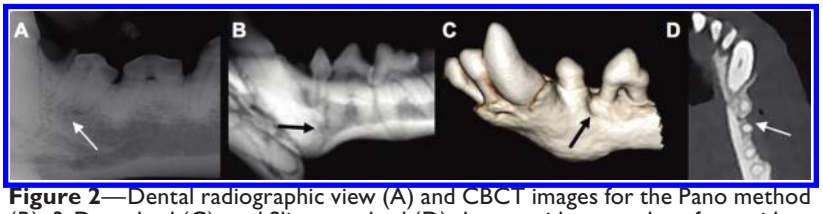

Figure 2—Dental radiographic view (A) and CBCT images for the Pano method (B), 3-D method (C), and Slices method (D) that provide examples of poor identification (grade = 1; scale, 0 to 3) for the left middle mental foramen (arrow), as defined by difficulty in identifying and outlining that anatomic landmark.

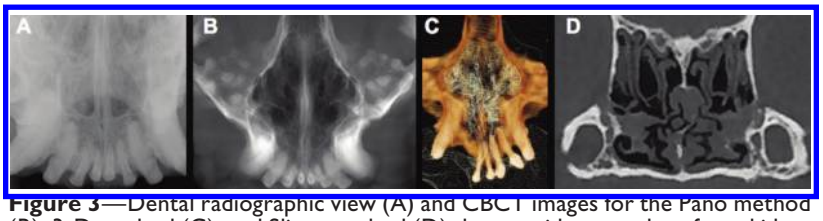

Figure 3—Dental radiographic view (A) and CBCT images for the Pano method (B), 3-D method (C), and Slices method (D) that provide examples of good identification (grade = 2; scale, 0 to 3) for the nasal turbinates, as defined by the ability to identify that anatomic landmark but difficulty in clearly outlining it.

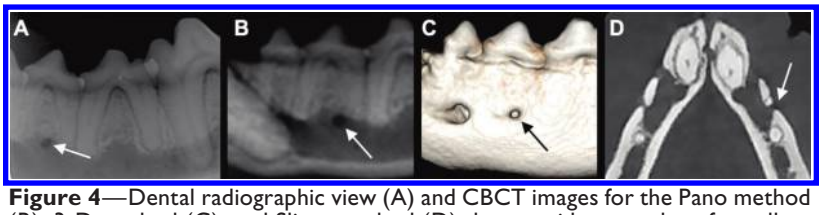

Figure 4—Dental radiographic view (A) and CBCT images for the Pano method (B), 3-D method (C), and Slices method (D) that provide examples of excellent identification (grade = 3; scale, 0 to 3) for the left caudal mental foramen (arrow), as defined by the ability to identify and clearly outline that anatomic landmark.

Semiquantitative scoring was used for each imaging method. Scoring was on a scale of 0 to 3 as follows: 0 = inability to identify the anatomic landmark **(Figure 1)**, 1 = poor identification of landmark **(Figure 2)**, 2 = good identification of landmark **(Figure 3)**, and 3 = excellent identification of landmark **(Figure 4)**. Mean score for each anatomic landmark was calculated for each imaging method.

One observer was calibrated by the other investigators to ensure appropriate software handling and image scoring. Findings for all 4 methods were recorded separately by the calibrated observer without reference to each patient's medical record to limit biased interpretation. Final scores were obtained by consensus of the investigators, who agreed on 1 interpretation for each finding. Mean score of a method was calculated for each landmark and as a total for each imaging method as a whole and was reported as poor (mean score < 1), moderate (mean score ≥ 1 and < 2), good (mean score ≥ 2 and < 3), or excellent (mean score = 3).

Slices method—Each skull was oriented by use of the CBCT software to properly align the Cartesian coordinate systems of the CBCT scanner to the sagittal, transverse, and dorsal planes of the patient. Thus, each point of the skull was assigned a specific position within the tridimensional space by use of 3 coordinates that could then be recognized by the CBCT software for further image manipulation. The sagittal, transverse, and dorsal slices in combination with custom cross sections were evaluated with the preset software settings for dental use and hard sharpening of the contrast.

3-D method—Tridimensional rendering is a volume-rendering technique whereby the entire volume of a CBCT scan is composed into 1 block of data, which then can be selectively displayed. The volume-rendering algorithm we used involved all acquired data and assigned voxels to various colors and transparency values (on the basis of their attenuation values) to enhance discrimination among structures. The volume-rendering technique allows users to adjust the display characteristics of selected tissues types that have unique x-ray attenuation values. The software used for the study reported here provided 2 main settings (tooth and bone mode; **Figure 5**). To optimize and standardize evaluation of the skulls for the tooth mode, images were set to level and brightness of 2,000 and 0, opacity was set to 1 and 3, and the window and contrast were decreased to 6,000 and –0.25. For the bone mode, settings were adjusted to a level and brightness window in which the density for oral soft tissues was just excluded from being shown (level and brightness = 1,440 to 1,760 and 0.06 to 0.14), opacity was set to 7 and 8, and window and contrast were increased to 2,400 and 0.20. The clipping tool was used to evaluate the right and left sides of the skull as well as to separately evaluate the mandible and maxilla. Incrementally advancing deeper into the skull by removing (ie, clipping away) each slice was not performed. The 3-D images were rotated to enable evaluation of each skull from all sites and angles in both bone and tooth modes.

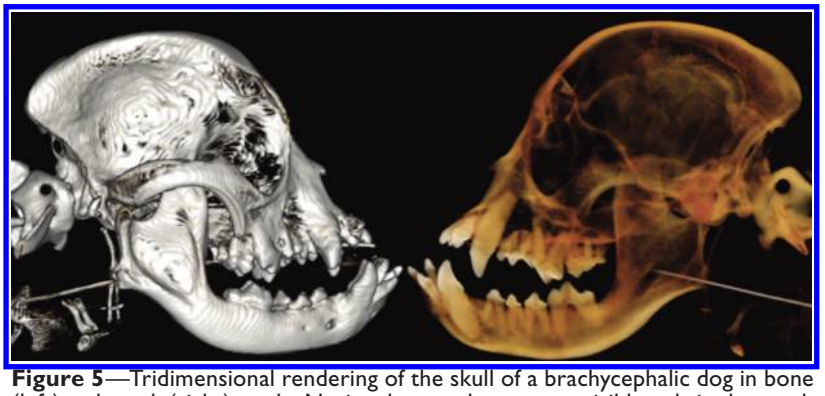

Figure 5—Tridimensional rendering of the skull of a brachycephalic dog in bone (left) and tooth (right) mode. Notice that tooth roots are visible only in the tooth mode, whereas other anatomic landmarks are more visible in the bone mode.

Pano method—Because of the morphology of brachycephalic skulls and the abundance of anatomic structures confined to a small area, the standard panoramic view was not sufficient for evaluation of the orofacial anatomy **(Figure 6)**. Instead, orientation of the skull was adjusted accordingly, and multiple reconstructed panoramic views with optimized plane location, shape, and thickness were created to enable us to obtain the full benefit of truly parallel imaging **(Figure 7)**.

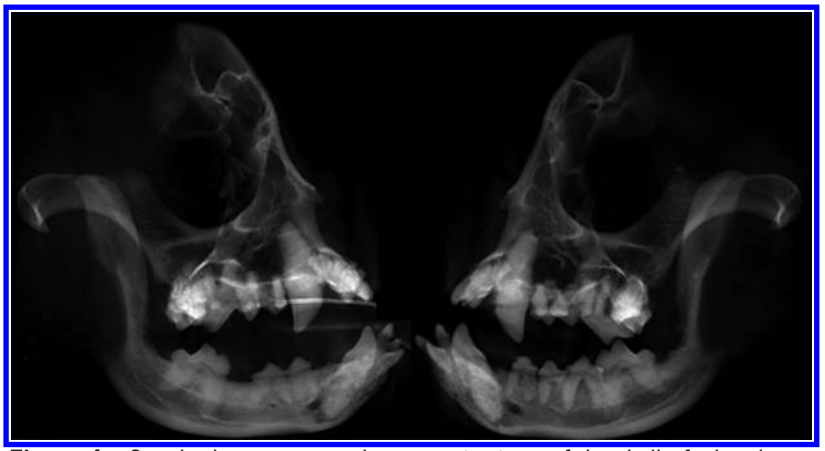

Figure 6—Standard reconstructed panoramic views of the skull of a brachycephalic dog in left lateral (left) and right lateral (right) recumbency. Notice the inability to exploit the full potential of lateral radiographs for evaluation of anatomic landmarks.

Statistical analysis

Descriptive statistics and mean scores were reported as mean ± SD. Scores from all patients for each ana-

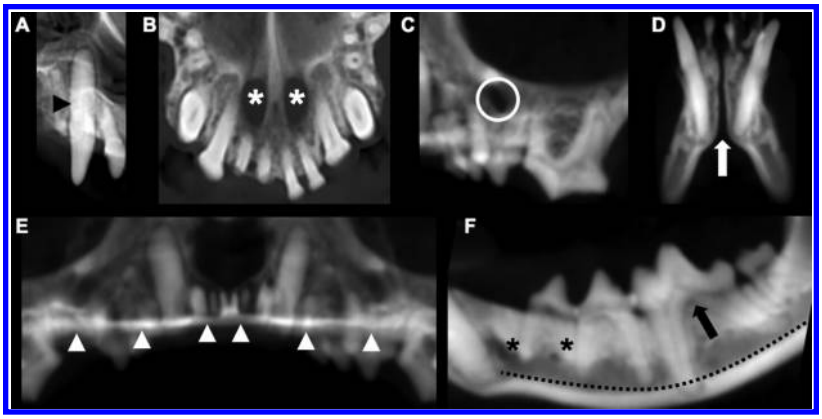

Figure 7—The CBCT optimized reconstructed panoramic views for the right maxillary canine tooth (black arrowhead; A), palatine fissures (white asterisks; B), left infraorbital foramen (white circle; C), mandibular symphysis (white arrow; D), plane of the hard palate (white arrowheads; E), and left middle and caudal mental foramina (black asterisks), left mandibular canal (black dotted line), and left mandibular first molar tooth (black arrow; F) in a brachycephalic dog.

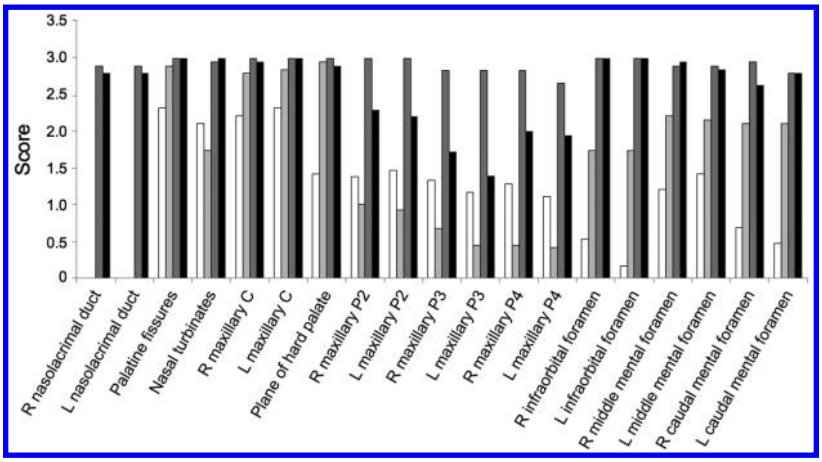

Figure 8—Mean score for each of 19 anatomic landmarks that differed significantly ($P < 0.05$) among the Rad method (white bars) and the 3 CBCT methods (Pano method [light gray bars], 3-D method [dark gray bars], and Slices method [black bars]) for evaluation of brachycephalic dogs. Scores were assigned by use of a scale of 0 to 3 as follows: 0 = inability to identify the anatomic landmark, 1 = poor identification of landmark, 2 = good identification of landmark, and 3 = excellent identification of landmark. C = Canine tooth. L = Left. P2 = Second premolar tooth. P3 = Third premolar tooth. P4 = Fourth premolar tooth. R = Right.

tomic landmark and each imaging method were used to calculate the overall mean ± SD. The Friedman test was used to evaluate differences in diagnostic yield of the mean scores for the Rad and 3 CBCT methods. When this test led to the finding of significant differences between at least 2 methods, the Wilcoxon signed rank test was used with the Bonferroni-Holm multiple comparisons adjustment to determine significant differences among each of the 6 possible pairs of diagnostic methods. Significance was set at values of $P < 0.05$.

Results

Animals

Nineteen dogs (12 males [11 castrated and 1 sexually intact] and 7 females [6 spayed and 1 sexually intact]) were included in the study. Breeds included French Bulldog (n = 4), Shih Tzu (3), Pekingese (3), Japanese Chin (3), Pug (2), English Bulldog (1), and Boston Terrier (1); there were also 2 mixed-breed dogs (Shi Tzu–Pekingese cross). Mean ± SD age of the dogs was 7.36 ± 3.65 years (range, 8 months to 14 years), mean body weight was 8.23 ± 5.13 kg (range, 2.2 to 25 kg), and mean skull index was 0.96 ± 0.09 (range, 0.81 to 1.14).

Overall scores

Mean scores for each anatomic landmark and each imaging method were calculated **(Figure 8)**. Of the 26 predefined oral anatomic landmarks, 7 mandibular landmarks were excluded from further statistical analysis because of a lack of significant differences among the imaging methods, as confirmed by results of the Friedman test. The 7 excluded landmarks were the mandibular symphysis, right and left mandibular canine teeth, right and left mandibular first molar teeth, and right and left mandibular canals. All combination pairs among the RAD method and 3 CBCT software modules for the 19 remaining anatomic landmarks were statistically compared **(Table 1)**.

Rad method

Compared with results for the Pano method, scores for the Rad method were significantly higher for 4 of 19 anatomic landmarks, which represented 4 of the 8 teeth selected for identification (right and left maxillary third and fourth premolar teeth). In addition, Rad scores were higher, although not significantly, for the right and left maxillary second premolar teeth and the nasal turbinates. The Rad scores were significantly lower for all anatomic landmarks, except for 1 (left maxillary third premolar tooth), when compared with scores for the 3-D method and for all 19 anatomic landmarks when compared with scores for the Slices method. Mean Rad score was poor for 6 anatomic landmarks, moderate for 9 anatomic landmarks, and good for 4 anatomic landmarks. Overall mean score for the Rad method was 1.68, which indicated a moderate ability for use in identification of anatomic landmarks.

Pano method

Scores for the Pano method were significantly higher than those for the Rad method for the palatine fissures, maxillary canine teeth, plane of the hard palate, right and left infraorbital foramina, and right and left caudal mental foramina, which represented 8 of

Table 1—Results of the Wilcoxon signed rank test for all 6 possible pairs of diagnostic methods for evaluation of anatomic landmarks in the skulls of brachycephalic dogs.

Variable	Rad vs Slices	Rad vs 3-D	Rad vs Pano	Pano vs Slices	Pano vs 3-D	Slices vs 3-D
Right nasolacrimal duct	< 0.001	< 0.001	1.000	< 0.001	< 0.001	0.618
Left nasolacrimal duct	< 0.001	< 0.001	1.000	< 0.001	< 0.001	0.618
Palatine fissures	0.003	0.003	0.003	0.157	0.157	1.000
Nasal turbinates	< 0.001	< 0.001	0.334	< 0.001	< 0.001	0.317
Right maxillary canine tooth	< 0.001	0.001	0.006	0.084	0.083	0.317
Left maxillary canine tooth	0.001	0.001	0.011	0.158	0.158	1.000
Plane of the hard palate	< 0.001	< 0.001	< 0.001	0.317	1.000	0.317
Right maxillary second premolar tooth	< 0.001	0.006	0.056	< 0.001	0.006	0.009
Left maxillary second premolar tooth	< 0.001	0.003	0.070	< 0.001	0.002	0.002
Right maxillary third premolar tooth	< 0.001	0.030	0.016	< 0.001	0.002	< 0.001
Left maxillary third premolar tooth	< 0.001	0.189	0.003	< 0.001	0.006	< 0.001
Right maxillary fourth premolar tooth	< 0.001	0.002	0.002	< 0.001	< 0.001	0.001
Left maxillary fourth premolar tooth	< 0.001	0.004	0.007	< 0.001	< 0.001	0.003
Right infraorbital foramen	< 0.001	< 0.001	0.003	< 0.001	< 0.001	1.000
Left infraorbital foramen	< 0.001	< 0.001	< 0.001	< 0.001	< 0.001	1.000
Right middle mental foramen	< 0.001	< 0.001	0.024	0.028	0.009	0.970
Left middle mental foramen	0.002	0.003	0.103	0.005	0.009	0.317
Right caudal mental foramen	< 0.001	< 0.001	0.007	0.009	0.026	0.084
Left caudal mental foramen	< 0.001	< 0.001	0.002	0.009	0.009	0.608

The diagnostic methods were dental radiography (Rad) and CBCT with 3 software modules (serial CBCT slices and custom cross sections [Slices], tridimensional rendering [3-D], and reconstructed panoramic views [Pano]).

Results reported are *P* values; values < 0.05 were considered significant.

19 predefined anatomic regions. The Pano scores were significantly lower than scores for the 3-D and Slices methods for 14 of 19 anatomic landmarks. The Pano scores were lower for the right and left nasolacrimal duct, nasal turbinates, right and left maxillary second through fourth premolar teeth, right and left infraorbital foramina, left middle and caudal mental foramina, and right middle mental foramen, compared with 3-D scores; Pano scores were lower for the right caudal mental foramen, compared with Slices scores. Mean Pano score was poor for 5 anatomic landmarks, moderate for 6 anatomic landmarks, and good for 8 anatomic landmarks. Overall mean score for the Pano method was 1.65, which equaled a moderate ability for use in the identification of anatomic landmarks.

3-D method

Scores for the 3-D method were significantly higher than scores for the Rad method for 16 of 19 anatomic landmarks; they also were higher, but not significantly so, for another anatomic landmark. In comparison to scores for the Pano method, 3-D scores were significantly higher for 11 of 19 anatomic sites; scores for the 3-D method were the highest in 7 of the regions. In 5 of those 7 regions, Slices scores were similar to 3-D scores, but 3-D scores were significantly lower than Slices scores for 6 anatomic landmarks, which represented all maxillary premolar teeth evaluated in the study. The 3-D method had the highest scores for 2 locations (nasal turbinates and right middle mental foramen), but not significantly so. Evaluation of the 3-D method for use in identification of anatomic landmarks revealed a score of moderate for 3 anatomic landmarks, good for 11 anatomic landmarks, and excellent for 5 anatomic landmarks. Overall mean 3-D score was 2.59, which resulted in an overall good identification score for anatomic landmarks.

Slices method

For all 19 predefined anatomic landmarks with significant differences among the methods, Slices scores were highest for 17 of the anatomic landmarks, compared with scores for the Rad, Pano, and 3-D methods. Compared with Rad scores, Slices scores were significantly higher for all 19 anatomic landmarks. Compared with Pano scores, Slices scores were significantly higher for 14 anatomic landmarks and higher, but not significantly so, for the other 5 anatomic landmarks. The Slices scores were significantly higher than 3-D scores for 6 anatomic landmarks and higher, but not significantly so, than 3-D scores for 6 other anatomic landmarks. Overall, mean Slices score was good for 11 anatomic landmarks and excel-

lent for 8 anatomic landmarks, which resulted in the highest mean score (2.77) for any of the methods.

Discussion

The objective of the study reported here was to investigate the use of CBCT as an imaging modality for the evaluation of anatomic landmarks of brachycephalic dogs in veterinary dentistry and oral surgery. In the present study, CBCT was an efficient imaging modality that was dependent on optimizing the software, which had been developed for the human skull, for the evaluation of brachycephalic dog skulls. Furthermore, given the unique skull configuration of brachycephalic dogs with the inherent crowding and rotation of teeth, CBCT had a higher diagnostic yield than did dental radiography for the evaluation of anatomic landmarks.

The standard panoramic view was deemed unfit for evaluation of the entire skull of brachycephalic dogs because the target anatomic landmarks were outside the curved plane of the section or there was superimposition of anatomic structures adjacent to the target anatomic landmarks within the plane of section. Therefore, multiple standardized additional views were used to enable us to exploit the benefits of truly parallel imaging without overlap of numerous anatomic structures, as would be the case with lateral skull radiographs. Although the present study did not represent 1 panoramic view per se and the value of the reconstructed panoramic views was limited, some of the optimized reconstructed panoramic images proved useful and superior to intraoral radiographs, such as for evaluation of the palatine fissures, maxillary canine teeth, plane of the hard palate, right and left infraorbital foramina, and right and left caudal mental foramina.

Anatomic landmarks excluded from further statistical analysis (eg, the mandibular canal) could be identified similarly well by use of the Rad method and the 3 CBCT methods; however, the scoring system for the present study was based on identification alone. Location (lingual vs buccal) or detail provided was not analyzed. Authors of a study[4] conducted to characterize the mandibular canal in brachycephalic dogs by use of conventional CT suggested that CBCT should be equally or better suited for a more detailed assessment of these important structures.

Studies conducted in veterinary[15] and human[16] dentistry found that CBCT imaging is superior to intraoral dental radiography with regard to general criteria such as duration of examination, anesthesia time, radiation exposure, and associated risks for patients. Authors of multiple morphometric studies[10,16,17] further concluded that a tridimensional imaging modality, such as CBCT, is better suited for identification of anatomic landmarks than are 2-D imaging modalities, such as dental radiography. It was anticipated that both the Slices and 3-D methods would have higher scores for identification of maxillofacial foramina, given the nature of the software modules.[18,19] The distinct difference between the Pano and Rad methods for identification of these structures can be deduced to be the oblique angle used for dental radiography, which leads to distortion and overlap between tooth roots and foramina, whereas these structures were separated by the parallel imaging provided with the Pano method. The nasolacrimal ducts were not visible for the Rad or Pano methods, which likely was associated with the fact that these structures are foramina rather than ducts, at least in the evaluated brachycephalic dogs. Similar findings have been reported for the description of the nasolacrimal draining system in brachycephalic cats.[20]

In the present study, teeth selected for identification were assessed in their entirety, whereas in humans, CBCT evaluations are primarily focused on specific areas of dental pathological conditions, such as the periapical region, pulp cavity, or occlusal surface. Because of the severe overlap of anatomic structures in the region of the maxillary premolar teeth for the Rad, Pano, and 3-D methods, it was not surprising to find significantly improved diagnostic yield for the Slices method for all evaluated teeth in that region, which confirmed the findings of a previous study.[15] However, the fact that similar results would also be found for the maxillary canine teeth was rather unexpected because overlap of anatomic structures is limited in that region. The finding was further intriguing because even Pano scores were higher for the maxillary canine teeth when compared with scores for the Rad method, which raised the question of whether the bisecting angle used for dental radiographs might obscure anatomic detail and, potentially, also associated pathological changes in brachycephalic breeds. Investigators of a recent veterinary study[21] evaluated visibility of tooth roots in medium-sized mesaticephalic dogs and compared single-detector with multidetector row CT. The authors of that study[21] concluded that a slice thickness of ≤ 1 mm together with a moderate enhancement filter was suitable for root identification and that thinner slices should be chosen for small dogs, cats, and rabbits. Although the investigators of that study did not compare CT images and dental radiographs, the results indicated that slice thickness is of importance when evaluating teeth and dental disorders, which would make CBCT better suited than conventional CT. For the chosen fields of view, the CBCT unit[c] used in the present study produced images with a resolution of 150 to 250 µm/isotropic voxel, compared with the dental radiographs obtained by use of a digital intraoral imaging system[b] that provided a resolution of 55.5 µm/pixel. This difference in resolution was apparent when enlarging a specific area. In particular, the sharp contour and outline of the dental lamina dura provided by intraoral radiography could not be met by CBCT imaging. Despite the superior resolution of dental radiographs, the ability to evaluate transverse, sagittal, and dorsal slices; to use serial multiplanar reconstructions and curved planar reformations; and to provide indirect volume rendering in tooth and bone mode by use

of the CBCT software offered important advantages. The overall success of CBCT reported in the present study indicated that the structural complexity of the skull of brachycephalic dogs was responsible for difficulties in evaluation of dental radiographs and that the overall diagnostic yield did not depend on resolution but, instead, depended primarily on unobstructed visibility of these structures. The clear advantage of CBCT images and multiplanar reconstruction lies in the ability to triangulate a landmark (ie, simultaneously viewing the same point in 3 planes), which allows for identification as well as spatial localization of anatomic structures. The margin of error for use of this technique on CBCT images has been determined to be submillimeter values.[22]

Cone-beam CT is commonly used for endodontic and orthodontic applications as well as implant planning for human dentistry and maxillofacial surgery. In fact, CBCT is already so well established that the latest CBCT-related studies no longer attempt to prove its superiority to conventional radiography, but instead use CBCT-derived images as the criterion-referenced standard for the localization and description of anatomic landmarks or for postoperative quality assessment of endodontic procedures.[18,19,23–28] However, CBCT has not yet reached similar status in veterinary dentistry.

The equipment for dental radiography is fairly affordable for veterinary practices, but CBCT scanners are expensive diagnostic tools with highly specific indications for use. When compared with conventional CT, the maximum field of view for CBCT is limited and only allows for evaluation of the entire skull of small to medium-sized dogs. However, when restricted to the oral cavity, large dogs can also be evaluated. Furthermore, with upgraded stitching software, entire skull images of large-breed dogs can be obtained. In addition, CBCT is optimized to depict maxillofacial hard tissues, and it is generally accepted that it does not provide sufficient soft tissue detail.[29] Despite the poorer soft tissue contrast of CBCT, compared with that of conventional CT, evaluation of the soft tissue is still possible. A study[30] to evaluate maxillofacial soft tissue by IV administration of iodinated contrast media and CBCT was conducted with rabbits. Authors of that study[30] concluded that small, strongly contrast-enhancing lesions and anatomic structures, such as blood vessels, can be detected. However, the use of contrast administration in dogs and cats for evaluation of maxillofacial soft tissue–associated diseases (eg, tumors, abscesses, or cysts) by use of CBCT has not yet been described.

The present study had some limitations. Comparison of diagnostic yield among the Rad method and CBCT methods for selected anatomic landmarks, such as the nasolacrimal ducts or infraorbital foramina, might seem biased. However, only clinically relevant structures were selected. The limitations of dental radiography have been described.[10] Nevertheless, the inferiority of the Rad method in the present study may also have reflected diagnostic shortcomings in the evaluation of dental disorders for which dental radiography currently represents the diagnostic criterion-referenced standard in veterinary medicine.

The goal of the study reported here was to quantitatively assess the ability to use conventional dental radiography and CBCT and 3 software modules to identify important anatomic landmarks and dental disorders in brachycephalic dogs. For the conditions of this study, it can be concluded that our hypothesis was confirmed. Results of this study should encourage exploration of potential further applications of CBCT in veterinary dentistry.

Acknowledgments

Supported by the University of California-Davis Center for Companion Animal Health.

Funding sources did not have any involvement in the study design, data analysis and interpretation, or writing and publication of this manuscript. The authors did not have any conflicts of interest with the sources of materials or companies described in this manuscript.

The authors thank John Doval for assistance with the figures and Megan Loscar, Monica Calder, and Kimi Kan-Rohrer for preparation of the images for review.

Footnotes

a. Siemens Sirona Heliodent MD, Sirona Dental Systems Inc, Long Island City, NY.
b. ScanX, Air Techniques, Melville, NY.
c. NewTom QR s.r.l., NewTom, Verona, Italy.
d. ASUS PB278Q 27-inch, ASUSTeK Computer Inc, Taipei, Taiwan.
e. Metron-Dental 7.40.34.0, Epona Tech LCC, Paso Robles, Calif.
f. InVivo5 dental application, Anatomage Inc, San Jose, Calif.

References

1. Fox MW. Developmental abnormalities of the canine skull. *Can J Comp Med Vet Sci* 1963;27:219–222.
2. Heidenreich D, Gradner G, Kneissl S, et al. Nasopharyngeal dimensions from computed tomography of Pugs and French Bulldogs with brachycephalic airway syndrome. *Vet Surg* 2016;45:83–90.
3. Hennet PR, Harvey CE. Craniofacial development and growth in the dog. *J Vet Dent* 1992;9:11–18.
4. Martinez LA, Gioso MA, Lobos CM, et al. Localization of the mandibular canal in brachycephalic dogs using computed tomography. *J Vet Dent* 2009;26:156–163.
5. Meola SD. Brachycephalic airway syndrome. *Top Companion Anim Med* 2013;28:91–96.
6. Verstraete FJM, Zin BP, Kass PH, et al. Clinical signs and histologic findings in dogs with odontogenic cysts: 41 cases (1995–2010). *J Am Vet Med Assoc* 2011;239:1470–1476.
7. Evans HE, de Lahunta A. The skeleton. In: *Miller's anatomy of the dog*. 4th ed. St Louis: Elsevier Saunders, 2013;80–157.
8. Verstraete FJM, Kass PH, Terpak CH. Diagnostic value of full-mouth radiography in dogs. *Am J Vet Res* 1998;59:686–691.
9. Verstraete FJM, Kass PH, Terpak CH. Diagnostic value of full-mouth radiography in cats. *Am J Vet Res* 1998;59:692–695.
10. Adams GL, Gansky SA, Miller AJ, et al. Comparison between traditional 2-dimensional cephalometry and a 3-dimensional approach on human dry skulls. *Am J Orthod Dentofacial Orthop* 2004;126:397–409.
11. American Association of Endodontists. Cone beam-computed tomography in endodontics. Available at: www.aae.org/uploadedfiles/publications_and_research/endodontics_colleagues_for_excellence_newsletter/ecfe%20summer%2011%20final.pdf. Accessed Dec 9, 2015.
12. Tyndall DA, Rathore S. Cone-beam CT diagnostic applica-

tions: caries, periodontal bone assessment, and endodontic applications. *Dent Clin North Am* 2008;52:825–841.
13. Kapila S, Conley RS, Harrell WE Jr. The current status of cone beam computed tomography imaging in orthodontics. *Dentomaxillofac Radiol* 2011;40:24–34.
14. Verstraete FJM. Dental radiographic technique for the dog and cat. Available at: www.avdc.org/Rad_tech_description.pdf. Accessed Dec 13, 2016.
15. Roza MR, Silva LA, Barriviera M, et al. Cone beam computed tomography and intraoral radiography for diagnosis of dental abnormalities in dogs and cats. *J Vet Sci* 2011;12:387–392.
16. Lofthag-Hansen S. Cone beam computed tomography radiation dose and image quality assessments. *Swed Dent J Suppl* 2010;209:4–55.
17. Bar-Am Y, Pollard RE, Kass PH, et al. The diagnostic yield of conventional radiographs and computed tomography in dogs and cats with maxillofacial trauma. *Vet Surg* 2008;37:294–299.
18. Blacher J, Van DaHuvel S, Parashar V, et al. Variation in location of the mandibular foramen/inferior alveolar nerve complex given anatomic landmarks using cone-beam computed tomographic scans. *J Endod* 2016;42:393–396.
19. Carruth P, He J, Benson BW, et al. Analysis of the size and position of the mental foramen using the CS 9000 cone-beam computed tomographic unit. *J Endod* 2015;41:1032–1036.
20. Schlueter C, Budras KD, Ludewig E, et al. Brachycephalic feline noses: CT and anatomical study of the relationship between head conformation and the nasolacrimal drainage system. *J Feline Med Surg* 2009;11:891–900.
21. Esmans MC, Soukup JW, Schwarz T. Optimized canine dental computed tomography protocol in medium-sized mesaticephalic dogs. *Vet Radiol Ultrasound* 2014;55:506–510.
22. Kumar V, Ang D, Williams K, et al. Comparison of two cone beam computed tomography multiplanar reconstruction orientation protocols. *J Biomed Graph Comput* 2013;3:7–15.
23. Anbiaee N, Eslami F, Bagherpour A. Relationship of the gonial angle and inferior alveolar canal course using cone beam computed tomography. *J Dent (Tehran)* 2015;12:756–763.
24. Angel JS, Mincer HH, Chaudhry J, et al. Cone-beam computed tomography for analyzing variations in inferior alveolar canal location in adults in relation to age and sex. *J Forensic Sci* 2011;56:216–219.
25. Arora S, Hegde V. Comparative evaluation of a novel smartseal obturating system and its homogeneity of using cone beam computed tomography: in vitro simulated lateral canal study. *J Conserv Dent* 2014;17:364–368.
26. Gupta R, Dhingra A, Panwar NR. Comparative evaluation of three different obturating techniques lateral compaction, Thermafil and Calamus for filling area and voids using cone beam computed tomography: an invitro study. *J Clin Diagn Res* 2015;9:ZC15–ZC17.
27. Møller L, Wenzel A, Wegge-Larsen AM, et al. Comparison of images from digital intraoral receptors and cone beam computed tomography scanning for detection of voids in root canal fillings: an in vitro study using micro-computed tomography as validation. *Oral Surg Oral Med Oral Pathol Oral Radiol* 2013;115:810–818.
28. Nur BG, Ok E, Altunsoy M, et al. Evaluation of technical quality and periapical health of root-filled teeth by using cone-beam CT. *J Appl Oral Sci* 2014;22:502–508.
29. Ahmad M, Jenny J, Downie M. Application of cone beam computed tomography in oral and maxillofacial surgery. *Aust Dent J* 2012;57(suppl 1):82–94.
30. Kim MSKB, Choi HY, Choi YJ, et al. Intravenous contrast media application using cone-beam computed tomography in a rabbit model. *Imaging Sci Dent* 2015;45:31–39.

Appendix

Predefined anatomic landmarks evaluated in brachycephalic dogs by use of dental radiography and CBCT images for each of 3 software modules.

Right and left nasolacrimal ducts, right and left infraorbital foramina, right and left maxillary canine teeth, right and left maxillary second premolar teeth, right and left maxillary third premolar teeth, right and left maxillary fourth premolar teeth, right and left mandibular canine teeth, right and left mandibular first molar teeth, right and left middle mental foramina, right and left caudal mental foramina, right and left mandibular canals, mandibular symphysis, nasal turbinates, palatine fissures, and plane of the hard palate.